X-ray diffuse scattering in the icosahedral quasicrystal Al-Pd-Mn

Y. Zhang,[1] S. N. Ehrlich,[2] R. Colella,[1,*] M. Kopecky,[3] and M. Widom[4]
[1]*Department of Physics, Purdue University, West Lafayette, Indiana 47907-1396*
[2]*Brookhaven National Laboratory, NSLS, Upton, New York 11973*
[3]*Sincrotrone Trieste, SS 14-Km 163.5, Area Science Park, 34012 Basovizza - Trieste, Italy*
[4]*Department of Physics, Carnegie Mellon University, Pittsburgh, Pennsylvania 15213*
(Received 20 December 2001; published 19 September 2002)

Several isointensity contour plots of diffuse scattering around Bragg reflections have been obtained at 300 and 20 K on planar sections of reciprocal space perpendicular to twofold axes. The geometry of the experiments was such that circular contours were expected on the basis of elastic isotropy, demonstrated by the speed of sound being uniform in all directions. Instead, the profiles were markedly elongated along a twofold axis, a direct indication of scattering due to phason fluctuations. The $1/q^2$ dependence of diffuse scattering was verified in the neighborhood of the $(0\,4\,6\,0\,\bar{4}\,6)$ Bragg reflection, but not near the $(5\,3\,3\,3\,1\,\bar{1})$, a possible indication of lack of equilibrium in the phason fluctuations.

DOI: 10.1103/PhysRevB.66.104202 PACS number(s): 61.44.Br

I. INTRODUCTION

A perfectly periodic crystal, without lattice defects such as vacancies, interstitials, dislocations, thermal motion, etc., does not produce any diffuse scattering. The diffraction pattern of such a crystal consists of sharp and narrow Bragg peaks, and no scattering is visible between Bragg peaks. Strictly speaking, this statement is true for coherent scattering. If incoherent scattering is present, such as Compton scattering in the case of x rays, a continuous background may be present, whose variations in reciprocal space are quite smooth and do not correlate with the positions of the atoms in the crystal. Compton scattering is also inelastic, so it can be removed, at least in principle, by an energy analysis.

Even the most perfect crystals, such as silicon and germanium, with essentially no lattice defects, exhibit an appreciable amount of diffuse scattering. This is due to thermal vibrations, which cause the crystal to appear disordered. In fact, the time of flight of each individual x-ray photon through the crystal is much smaller than the period of thermal vibrations, so every phonon ''sees'' a different crystal, in which most of the atoms are out of their lattice positions. Thermal diffuse scattering (TDS) is temperature dependent, and is present even at $T=0$ K, due to the zero point energy.

In a perfect crystal such as silicon or germanium TDS would be the only source of diffuse scattering (apart from Compton scattering). But in a quasicrystal the situation is quite different because there is no periodicity, and some lattice disorder is present as an inherent feature of the crystal structure, which exhibits sharp Fourier components even in the absence of periodicity.

We decided to concentrate on icosahedral Al-Pd-Mn, because it is a very ''perfect'' quasicrystal, in the sense that it produces x-ray rocking curves extremely sharp (15–30 arcsec), comparable to those produced by germanium and silicon. Since diffuse scattering is quite sensitive to the atomic locations, we hope that this work will be useful for evaluating models which specify atomic locations in quasicrystals.

Our work is meant to expand and complement other diffuse scattering studies that have appeared recently in the literature of quasicrystals. Previous studies of x-ray diffuse scattering in icosahedral structures were done in an Al-Cu-Fe quasicrystal, the first high quality material that could be obtained in large size.[1,2] Extensive investigations of diffuse scattering from the icosahedral phase of Al-Pd-Mn were performed by de Boissieu *et al.*,[3] using elastic neutron scattering. This scattering, close to Bragg reflections, was mostly due to phason disorder. All data could be interpreted by making use of the elastic theory of quasicrystals, with two elastic constants. Detailed x-ray studies were performed more recently by Capitan *et al.*,[4] in which the effect of stoichiometry was investigated in detail.

More recently, Létoublon *et al.* further investigated the nature of diffuse scattering in Al-Pd-Mn by x-ray and neutron scattering,[5] and placed their intensity measurements on an absolute scale, in order to obtain the numerical values of the phason elastic constants. They also showed that diffuse scattering does not depend on lattice defects.

II. EXPERIMENT

The sample was the same as that used in a separate diffuse scattering experiment in which use was made of an imaging plate as a detector.[6] A detailed description of the specimen was given in Ref. 6, and it is partially reproduced here. The sample was a thin slice of $Al_{71.0}Pd_{20.5}Mn_{8.5}$ cut perpendicular to a twofold axis (within 0.25°), and diamond polished on both sides. The thickness was 0.385 mm, as measured with a micrometer. A perfect region was selected, in which a synchrotron beam from a perfect Si crystal monochromator would produce a sharp diffraction peak with no apparent broadening (about 20 arcsec wide or less). To make sure that the same crystal region was used in all experiments, the crystal was set against a thick copper plate with a 1.5-mm hole. The crystal and its specimen holder were placed inside of a closed circle refrigerator. We took two sets of data, at room temperature (300 K) and at 20 K. All data described in this paper were taken at the National Synchrotron Light Source (NSLS) of Brookhaven National Laboratory, on beam line

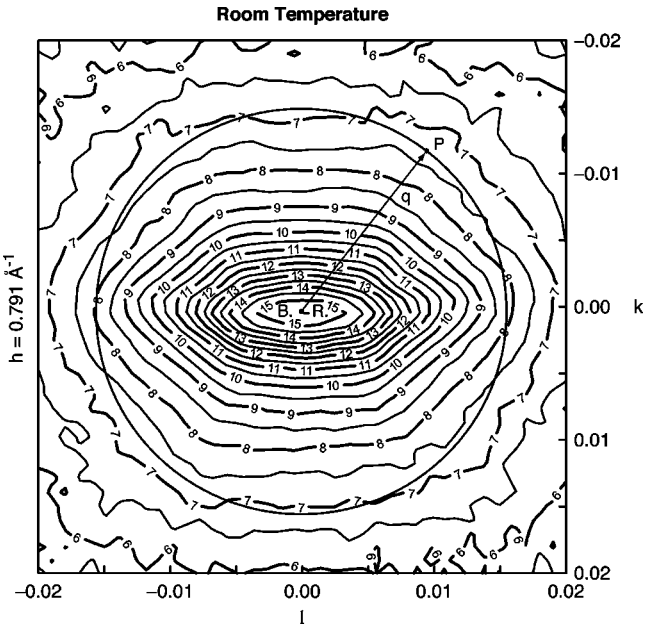

FIG. 1. Experimental contour profiles of diffuse scattering on the (k,l) plane. Units for the (hkl) axes are in Å^{-1}. The Bragg reflection $(4\,6\,0\,\bar{4}\,6\,0)$ is at the center of the plot. The numbers are intensities in arbitrary units, on a logarithmic scale (base 2).

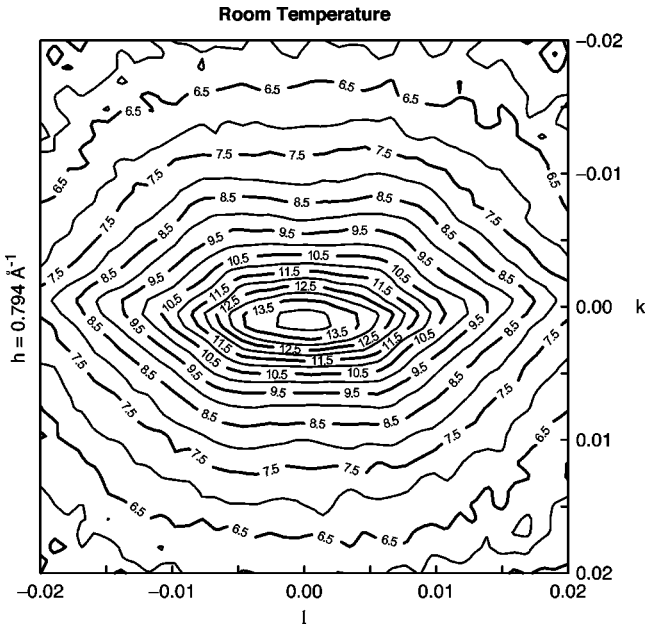

FIG. 2. The same as Fig. 1, except that the (k,l) plane is slightly off the Bragg reflection ($\Delta Q_x = 0.003$ Å^{-1}).

X18-A. The incident x-ray beam size was less than 1.0×1.0 mm^2. The x-ray energy was 17.4 KeV, corresponding to Mo-$K\alpha$, ($\lambda = 0.711$ Å). Polaroid photos were taken upstream and downstream with respect to the sample, to make sure that the x-ray beam was not blocked even partially by the sample holder for every change of orientation. All measurements were taken in a transmission geometry. A scintillation detector was used throughout all measurements. Typical scans were planar scans, on planes perpendicular to a twofold axis, in the neighborhood of a strong Bragg reflection, the $(4\,6\,0\,\bar{4}\,6\,0)$ ($Q_x = 0.790$, $Q_y = 0.0$, $Q_z = 0.0$; $M = 336$; $N = 208$). The conventions on the sixfold Miller indices notation, and the conversion to a three-dimensional (3D) reciprocal lattice, are those of Ref. 7. A reciprocal lattice vector Q is given by $Q = 2 \sin\theta/\lambda$. A typical 2D scan across the plane $Q_x = 0.790$ Å^{-1}, at room temperature, is shown in Fig. 1. A very similar plot was obtained at 20 K. As we depart a little from the Bragg reflection, ($Q_x = 0.793$ Å^{-1} and $\Delta Q_x = 0.003$ Å^{-1}), the isodiffusion contour profiles keep the same shape, albeit with a weaker intensity (Fig. 2). A plot taken at $\Delta Q_x = -0.003$ Å^{-1} (not shown here) is almost identical. While the earlier studies of diffuse scattering in quasicrystals[1,3–5] were done in the neighborhood of Bragg reflections, in this work we explored regions of the reciprocal space at some distance from the Bragg spots.

As we depart more from the Bragg reflection, the profiles acquire different shapes and the overall intensity becomes weaker and weaker. Figure 3, for example, corresponds to the plane $Q_x = 0.781$ Å^{-1} ($\Delta Q_x = -0.009$ Å^{-1}) and Fig. 4 corresponds to the plane $Q_x = 0.798$ Å^{-1} ($\Delta Q_x = +0.008$ Å^{-1}). Notice the lack of symmetry in the diffuse scattering around the Bragg reflection, for relatively large values of ΔQ_x. Such a lack of symmetry was not observed in proximity of the Bragg reflection. The same plots taken at 20 K were almost identical, except for a small increase of intensity, in rough agreement with a change in the Debye-Waller factor.[8]

III. DISCUSSION

All scans on planes perpendicular to the Q_x direction clearly show a twofold symmetry. This is to be expected, because the Q_x direction is a twofold axis. Let $G_{\|}$ be the

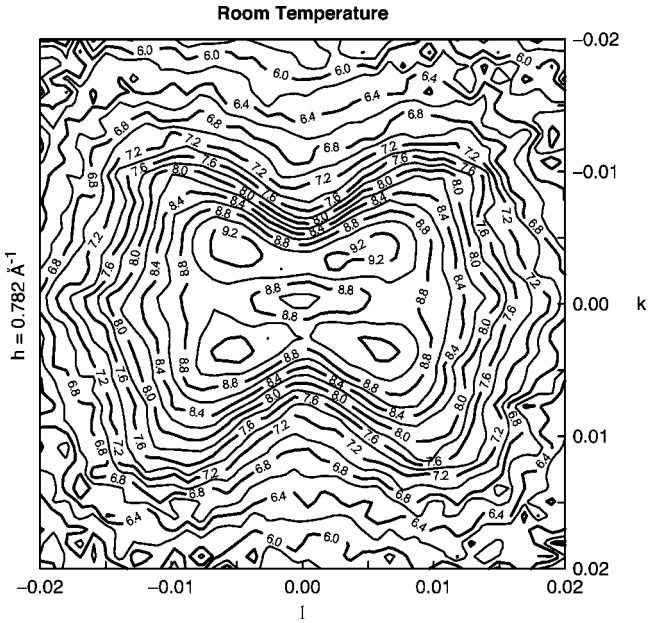

FIG. 3. The same as Figs. 1 and 2, except that $\Delta Q_x = -0.009$ Å^{-1}.

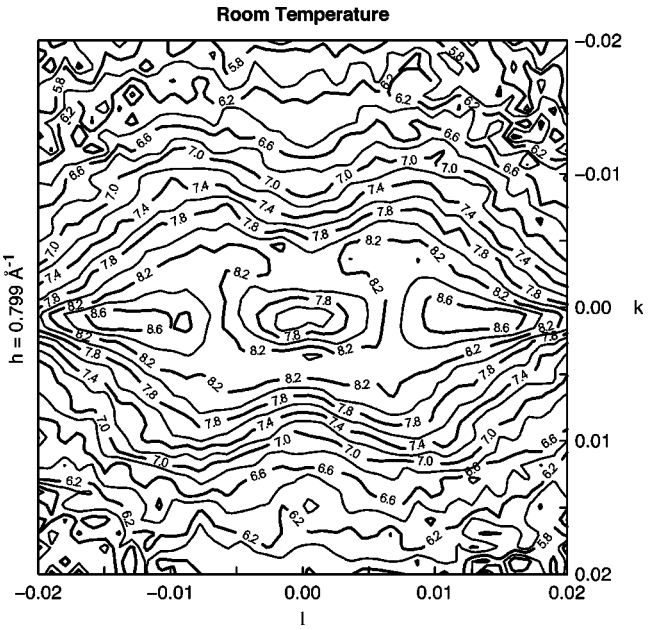

FIG. 4. The same as Figs. 1 and 2, except that $\Delta Q_x = +0.008$ Å^{-1}.

magnitude of the $(4\,6\,0\,\bar{4}\,6\,0)$ reciprocal lattice vector ($=0.790$ Å^{-1}). The scattering vector in our setup was perpendicular to the $Q_x = G_\parallel$ plane, when the Bragg reflection $(4\,6\,0\,\bar{4}\,6\,0)$ was excited, which would correspond to the central point of Fig. 1. The scattering vector was almost perpendicular to the plane of Fig. 1 at any other point of the figure. For example, the angle of the scattering vector with the plane of Fig. 1 would be about 88° at any of the four corners of the figure. It is then clear that the angle between the scattering vector and the plane of Fig. 1 is constant on any circular contour centered at the center, such as that shown in the figure.

Icosahedral quasicrystals are considered to be elastically isotropic, as a result of their symmetry properties. In fact, the speed of sound has been measured in several directions and found to be uniform within 100 parts per million.[9] Now, we know that the elastic properties of an isotropic medium can be described by means of two elastic constants, for example, the longitudinal and the shear speeds of sound. For quasicrystals, this has been shown by several authors.[10–12] We will adopt the view, in this paper, that quasicrystals can be described as isotropic media. For example, they can be described as crystals having cubic symmetry, in which the condition for isotropy,

$$c_{11} - c_{12} = 2c_{44}, \tag{1}$$

is satisfied. In fact, symmetry operations like those that lead to a reduction in the number of elastic constants, from 21 for a general solid with no symmetry, to 3 for a solid with cubic symmetry, can be used for a solid with icosahedral symmetry to reduce the number to 2. In the case of an isotropic solid, the dynamical equations for sound waves (for example, Eqs. 10.9 in Ref. 13) are simplified, and for *any* wave vector $\boldsymbol{k}$ there is one solution corresponding to a longitudinal wave,

$$v_l = \sqrt{c_{11}/\rho}, \tag{2}$$

where ρ is the density of the material and v_l is the longitudinal velocity), and two degenerate solutions corresponding to transverse waves of arbitrary polarizations:

$$v_t = \sqrt{c_{44}/\rho} \tag{3}$$

(where v_t is the transverse, or shear velocity). Consider now the expression for the first order x-ray diffuse scattering intensity, at a given point P in reciprocal space, for an isotropic monoatomic crystal. It can be derived from Eq. (11.36) of Ref. 14. A similar expression for quasicrystals is given in Ref. 15. The expression given here has been adapted to the experimental conditions under which the contour plot of Fig. 1 has been obtained.

$$I_1(\boldsymbol{S}/\lambda) = f^2 e^{-2M} \frac{kT}{V_c m} \cdot \left(\frac{|\boldsymbol{S}|^2/\lambda^2}{q^2} \right) \left(\frac{\cos^2\gamma}{v_l^2} + \frac{\sin^2\gamma}{v_t^2} \right), \tag{4}$$

where $\boldsymbol{S} = \hat{\boldsymbol{V}}_s - \hat{\boldsymbol{V}}_0$; $\hat{\boldsymbol{V}}_0$ is the incident beam unit vector; $\hat{\boldsymbol{V}}_S$ is the scattered beam unit vector; λ is the wavelength of the x rays; f is the atomic scattering factor; e^{-2M} is the Debye-Waller factor; k is the Boltzmann constant; v_l is the longitudinal sound velocity; v_t is the transverse sound velocity; T is the temperature; V_c is the volume of the unit cell; m is the atomic mass; $\boldsymbol{q}$ is the phonon wave vector, issued at Bragg reflection, terminating at point $P = \boldsymbol{S}/\lambda - \boldsymbol{G}_\parallel$; and γ is the angle between $\boldsymbol{S}$ and $\boldsymbol{q}$.

Consider now a point P on a circumference of arbitrary radius centered on the Bragg reflection in Fig. 1. As we go around the circle, the Q magnitude and the velocities v_l and v_t are constant. Therefore, the intensity is the same at any point on the circle. This would not be true in the plots of Ref. 3. It can easily be shown that second order diffuse scattering (two-phonon scattering) is also expected to be isotropic (see Sec. 1.6 in Ref. 14). An example of an isotropic solid giving circular contours of diffuse scattering is that of tungsten.[16]

It is therefore somewhat surprising to see the contours of Fig. 1 definitely departing from a circular shape. The reason for this is that a large fraction of diffuse scattering is due to phasons, whose velocities are not supposed to be isotropic.

The departure from circular symmetry visible in Fig. 1 can therefore be directly connected with the existence of phasons in Al-Pd-Mn, which can indeed produce anisotropic diffuse scattering,[15] as proved by the anisotropic ultrasonic attenuation observed by Amazit *et al.*[9] The question may be asked whether or not this lack of circular symmetry can also be observed around other Bragg reflections.

In a separate experiment, described in Ref. 6, we took diffuse scattering data using a technique called the ''monochromatic Laue method.'' This method simply consists of keeping a crystal stationary on a monochromatic x-ray beam, and recording the diffraction pattern on a flat film, (in our case, an imaging plate) perpendicular to the incident beam, placed downstream with respect to the crystal. In this way, each image corresponds to a spherical cap in reciprocal space being projected on a plane. Three-dimensional regions of

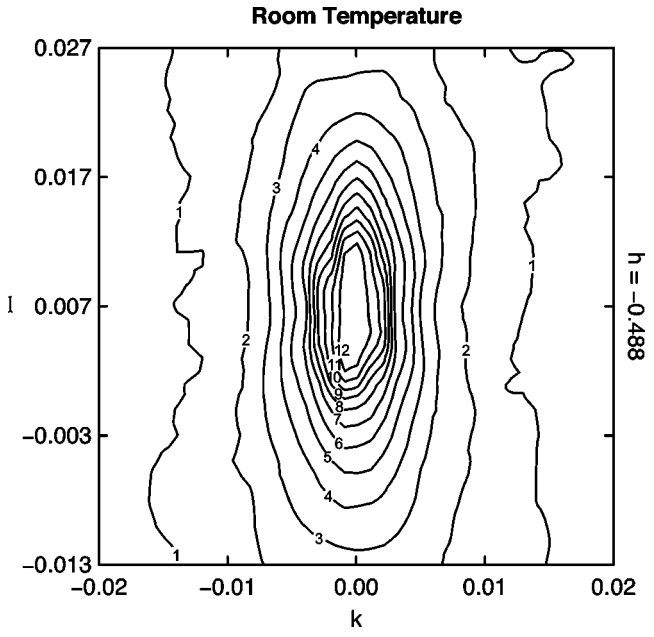

FIG. 5. Contour profiles of diffuse scattering on the (k,l) plane. The Bragg reflection $(\bar{2}\,4\,0\,2\,\bar{4}\,0)$ is at the center of the plot. Data taken with imaging plate, using the monochromatic Laue method.

reciprocal space can be explored by rotating the crystal around an axis perpendicular to the incident beam. Data were taken in several million data points. Two-dimensional scans on given planes in reciprocal space were then obtained by interpolation. Figure 5 shows a typical contour plot around the $(\bar{2}\,4\,0\,2\,\bar{4}\,0)$ Bragg reflection, also located on a twofold axis, with $Q_x=-0.4882$, $Q_y=0.0$, $Q_z=0.0$, $M=128$, and $N=80$. It is clear that the asymmetry persists. The shapes of the profiles in Fig. 5 are very similar to those of Fig. 1. This phason scattering is present around all Bragg reflections, most likely. This example shows the power and the convenience of image plates as two-dimensional detectors. Sizable three-dimensional regions of reciprocal space can be scanned in minutes, as opposed to the hours needed to obtain two-dimensional scans such as those of Figs. 1–5, obtained by counting point by point, using a scintillation counter.

IV. COMPARISON WITH THEORY

Since the oval shapes of the iso-intensity contour plots in Figs. 1 and 2 cannot be produced by phonon scattering, which would generate circular plots, we will attempt to analyze the data in Figs. 1–4 in terms of phason scattering. Compton scattering is also neglected in this analysis, because it is rather uniform over the regions depicted in Figs. 1–4.

Diffuse scattering from equilibrium phason fluctuations are governed by the form of the elastic free energy.[2,15,7] If we represent by $\mathbf{w}(\mathbf{q})$ the Fourier amplitude of a phason mode with wavevector $\mathbf{q}=(q_x,q_y,q_z)$, then the phason elastic free energy is

$$F=\frac{1}{2}\int\frac{d\mathbf{q}}{(2\pi)^3}\mathbf{w}(-\mathbf{q})\cdot\mathbf{C}(\mathbf{q})\cdot\mathbf{w}(\mathbf{q}), \tag{5}$$

where the "hydrodynamic matrix" $\mathbf{C}(\mathbf{q})=K_1\mathbf{C}_1(\mathbf{q})+K_2\mathbf{C}_2(\mathbf{q})$ with

$$\mathbf{C}_1(\mathbf{q})=\begin{pmatrix} q^2 & 0 & 0\\ 0 & q^2 & 0\\ 0 & 0 & q^2\end{pmatrix} \tag{6}$$

and

$$\mathbf{C}_2(\mathbf{q})=\begin{pmatrix} q^2/3+q_y^2/\tau-\tau q_z^2 & -2q_xq_y & -2q_xq_z\\ -2q_yq_x & q^2/3+q_z^2/\tau-\tau q_x^2 & -2q_yq_z\\ -2q_zq_x & -2q_zq_y & q^2/3+q_x^2/\tau-\tau q_y^2\end{pmatrix}. \tag{7}$$

Although the current experiments have been performed at $T=300$ K, and the phasons are presumably not in thermal equilibrium, we suppose that they are frozen into a configuration representative of equilibrium at some higher temperature.

The diffuse scattering intensity can be derived from the free energy [Eq. (5)] through Gaussian integration.[2,15,17] The resulting diffuse intensity at the point $\mathbf{Q}_\parallel=\mathbf{G}_\parallel+\mathbf{q}$ is proportional to

$$I_{\mathbf{G}}(\mathbf{q})=\mathbf{G}_\perp\cdot\mathbf{C}^{-1}(\mathbf{q})\cdot\mathbf{G}_\perp. \tag{8}$$

Here $\mathbf{G}_\parallel$ is a Bragg peak position, and $\mathbf{G}_\perp$ is its perpendicular space component. For the $(4\,6\,0\,\bar{4}\,6\,0)$ and $(\bar{2}\,4\,0\,2\,\bar{4}\,0)$ peaks, both $G_\parallel$ and $G_\perp$ lie along the x direction. Hence their intensities are given by the "11" element of $\mathbf{C}^{-1}$. In the plane perpendicular to $\mathbf{G}_\parallel$ we set $q_x=0$. The diffuse intensity is then

$$I_{\mathbf{G}}(q_y,q_z)=\frac{|\mathbf{G}_\perp|^2}{K_1(q_y^2+q_z^2)+K_2((-1/3-1/\tau)q_y^2+(1/3-\tau)q_z^2)}. \tag{9}$$

Figure 6 shows contours of this function. We set K2/K1$=-0.65$, a value slightly closer to the instability at K2/K1$=-3/4$ than reported in prior experiments by de Bois-

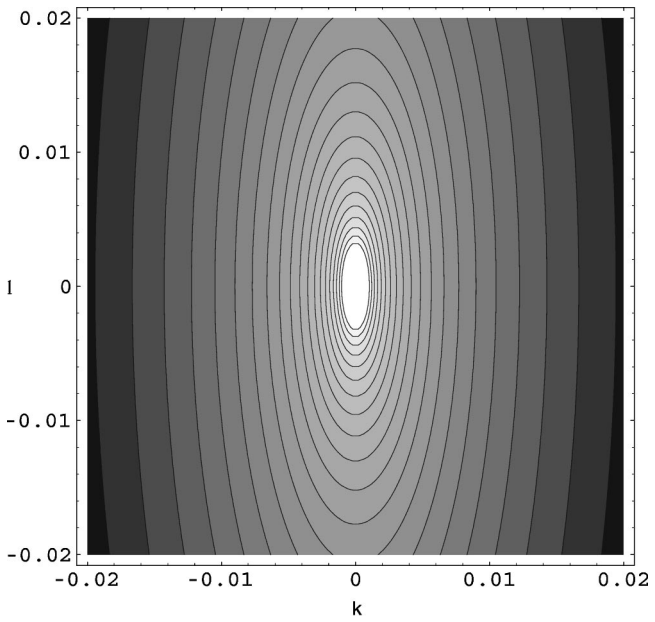

FIG. 6. Diffuse scattering plot on the (k,l) plane. The Bragg reflection $(4\,6\,0\,\bar{4}\,6\,0)$ is at the center of the plot. Units for the (hkl) axes are in Å^{-1}. Calculated from elasticity theory.

sieu *et al.*[3] Note the diffuse scattering contours are elongated in the q_z direction, with an aspect ratio similar to that seen in Figs. 1 and 5.

As we depart from the Bragg reflection (Figs. 3 and 4), the oval shape is lost. The calculated profile in Fig. 7 bears a striking resemblance with Fig. 4. We would be tempted to conclude that the agreement between theory and experiment persists at some distance from the Bragg reflection. The problem is that the theory predicts perfect symmetry with respect to the sign of q_x. In other words, the intensity given

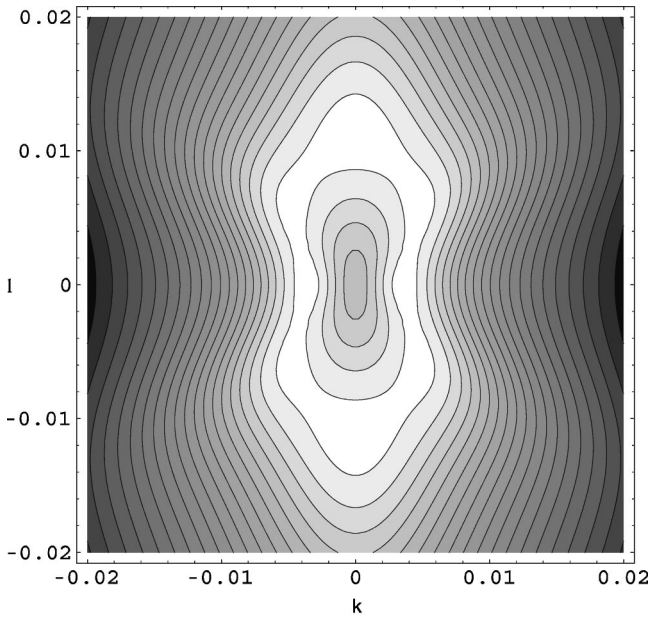

FIG. 7. The same as Fig. 6, except that the (k,l) plane is off the Bragg reflection ($\Delta Q_x = 0.008$ Å^{-1}).

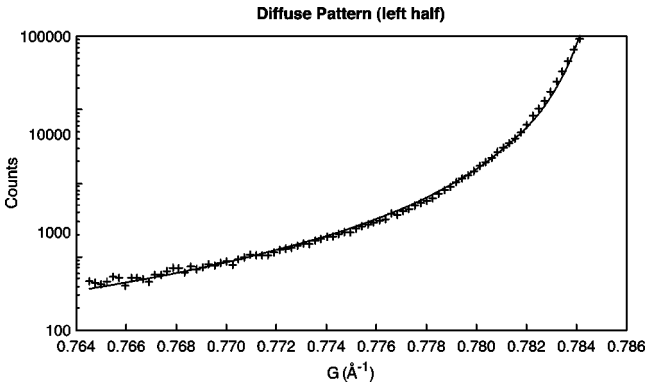

FIG. 8. Diffuse scattering near a Bragg reflection: the $(0\,4\,6\,0\,\bar{4}\,6)$. Its coordinates in reciprocal space are $Q_x = 0$, $Q_y = 0$, and $Q_z = 0.78995$ Å^{-1}. This was a scan along a straight line going through the Bragg reflection and the origin (a θ-2θ scan). Low-Q side. Values on abscissa are distances from the origin in reciprocal space.

by the equation for $I_{\mathbf{G}}(q_y, q_z)$ derived for $q_x \neq 0$ (not given here) is the same for $\pm q_x$. Such symmetry is indeed observed for planar plots located near the Bragg reflection ($q_x = \pm 0.003$ Å^{-1}). However, as we depart from the Bragg reflection (Figs. 3 and 4), the plots look quite different. The q_x values (-0.009 and $+0.008$) differ in magnitude by an amount corresponding to the experimental error. At the moment we have no explanation for the difference in the iso-intensity contour plots of Figs. 3 and 4. This subject deserves further study.

V. $1/Q^2$ DEPENDENCE OF DIFFUSE SCATTERING

Equation (4) shows that the diffuse scattering due to phonons should be proportional to $1/q^2$, where q is the phonon wave vector, defined by

$$\boldsymbol{S}/\lambda = \boldsymbol{G}_{\parallel} + \boldsymbol{q}, \tag{10}$$

where $\boldsymbol{S}/\lambda$ is the scattering vector and $\boldsymbol{G}_{\parallel}$ is the Bragg reflection under consideration. The general formula (11.36) in Ref. 14 does in fact predict a $1/q^2$ dependence. Equation (4) was obtained under the assumption of elastic isotropy. The same result applies to quasicrystals (see Eq. 1.15 in Ref. 15.). So it

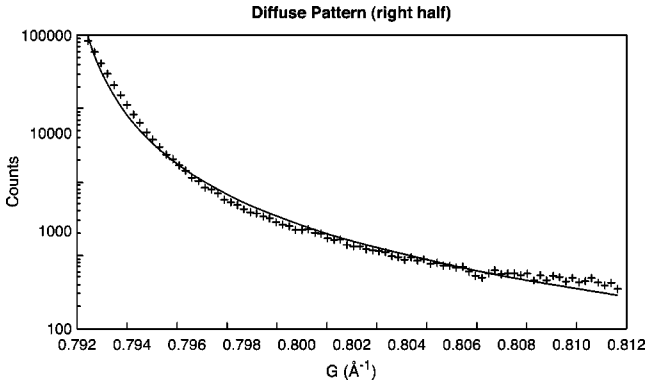

FIG. 9. The same as Fig. 8, except that this is the high-Q side.

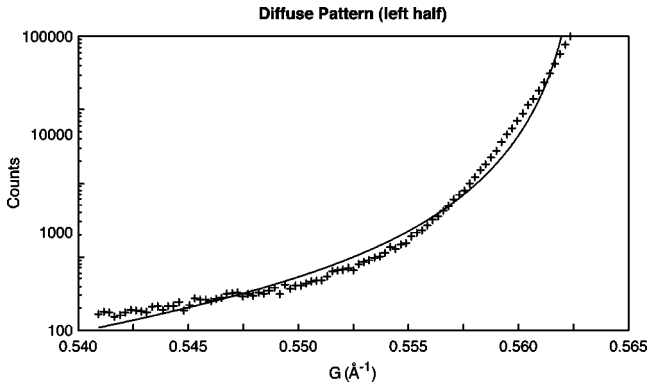

FIG. 10. Diffuse scattering near a Bragg reflection: the $(5\,3\,3\,3\,1\,\bar{1})$. Its coordinates in reciprocal space are: $Q_x = 0.244$ Å^{-1}, $Q_y = 0.488$ Å^{-1}, and $Q_z = 0.151$ Å^{-1}. This was a scan along a straight line going through the Bragg reflection and the origin (a θ-2θ scan). Low-Q side. Values on abscissa are distances from the origin in reciprocal space. Best fit is obtained with $1/q^{\alpha}$, with $\alpha = 2.24 \pm 0.03$.

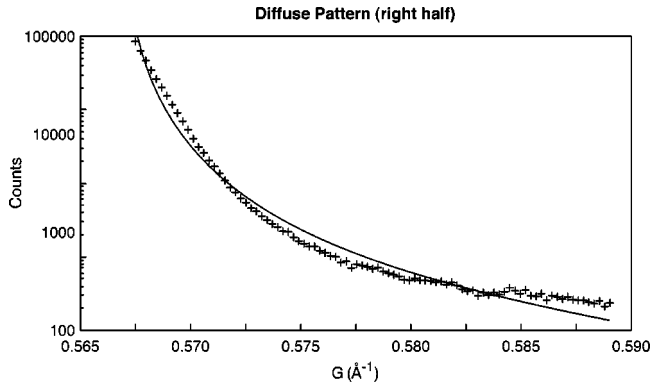

FIG. 11. The same as Fig. 10, except that this is the high-Q side, and $\alpha = 2.18 \pm 0.03$.

is interesting to verify this point. To answer this question we explored the environment of two Bragg reflections. We performed θ-2θ scans, which are along straight lines in reciprocal space, going through the origin and the relevant Bragg reflection. Portions of the scans are shown in Figs. 8 and 9. The relevant Bragg reflection is the $(0\,4\,6\,0\,\bar{4}\,6$; M=336, N=208). The $\boldsymbol{Q}$ components are $Q_x = 0.0$, $Q_y = 0.0$, and $Q_z = 0.790$ Å^{-1}. It is one of the strongest reflections, with $Q_{\perp} = 0.0272$ Å^{-1}. The variable in abscissa is the magnitude of the scattering vector $Q = |\boldsymbol{S}/\lambda|$. The two figures correspond to the two sides of the Bragg reflection. The solid lines represent fits to a $1/q^{\alpha}$ function. The exponent α is found to be 1.923 ± 0.020 on the low G side, and 2.077 ± 0.012 on the high G side. It is not clear whether or not the difference $\alpha - 2$ is significant. The $1/q^2$ behavior seems to be well established around the $(0\,4\,6\,0\,\bar{4}\,6)$ Bragg reflection.

However, if we look at the environment of another Bragg reflection, the $(5\,3\,3\,3\,1\,\bar{1})$, where $M = 172$ and $N = 108$, the situation is quite different. It is a rather weak reflection. The $\boldsymbol{Q}$ components are $Q_x = 0.244$ Å^{-1}, $Q_y = 0.488$ Å^{-1}, $Q_z = 0.151$ Å^{-1}, $Q_{\parallel} = 0.566$ Å^{-1}, and $Q_{\perp} = 0.0608$ Å^{-1}. Figures 10 and 11 again show the low and high values of Q, the scattering vector. The Bragg reflection is located at $Q = 0.566$ Å^{-1}. The solid curves represent the best possible fit to $1/q^{\alpha}$. The α values are 2.24 ± 0.03 on the low Q side, and 2.18 ± 0.03 on the high Q side. Clearly, there is no $1/q^2$ dependence around the $(5\,3\,3\,3\,1\,\bar{1})$. It could also be due to the fact that, while in a periodic crystal the Bragg reflections are widely spaced, the reciprocal space of a quasicrystal is uniformly filled with Bragg reflections, so there is no guarantee that diffuse scattering should vary as $1/q^2$. This apparent violation of the continuum elastic scattering theory[2,15] deserves further study. Perhaps the phason fluctuations are not properly in equilibrium at this low temperature. Another possibility is the effect of second order diffuse scattering.[18]

VI. CONCLUSIONS

Isodiffusion contour plots of diffuse scattering on planes perpendicular to a twofold axis have been obtained for the icosahedral quasicrystal Al-Pd-Mn. The scattering geometry was such that circular contours should have been obtained under the assumption of elastic isotropy. The fact that the profiles definitely depart from circumferences is a direct proof that phasons contribute a significant portion of the diffuse intensity.

The $1/q^2$ behavior has been observed to hold near the $(0\,4\,6\,0\,\bar{4}\,6)$ Bragg reflection, but not near the $(5\,3\,3\,3\,1\,\bar{1})$, a possible consequence of lack of equilibrium in the phason fluctuations at room temperature and below.

ACKNOWLEDGMENTS

The authors are indebted to Professor M. Widom for his many insights and clarifications on understanding diffuse scattering in quasicrystals. Thanks are due to M. de Boissieu and M. Boudard, who made available their program to calculate atomic sites in icosahedral Al-Pd-Mn quasicrystal, and to S. W. Kycia, who prepared the crystalline specimen at Iowa State University, under the supervision of Professor A. Goldman. The beamline X18-A at NSLS (Brookhaven) was funded by the U.S. Department of Energy (DOE) and the work at Purdue was funded by the National Science Foundation Grant 9625585-DMR.

*Corresponding author. Email address: colella@physics.purdue.edu

[1] M. Mori, T. Ishimasa, and Y. Kashiwase, Philos. Mag. Lett. **64**, 49 (1991).

[2] M. Widom, Philos. Mag. Lett. **64**, 297 (1991).

[3] M. de Boissieu, M. Boudard, B. Hennion, R. Bellissent, S. Kycia, A. Goldman, C. Janot, and M. Audier, Phys. Rev. Lett. **75**, 89 (1995).

[4] M. J. Capitan, Y. Calvayrac, A. Quivy, J. L. Joulaud, S. Lefebvre, and D. Gratias, Phys. Rev. B **60**, 6398 (1999).

[5] A. Létoublon, M. De Boissieu, M. Boudard, L. Mancini, J. Gastaldi, B. Hennion, R. Caudron, and R. Bellissent, Philos.

Mag. Lett. **81**, 273 (2001).
[6] M. Kopecky and R. Colella, J. Appl. Crystallog. **32**, 442 (1999).
[7] J. W. Cahn, D. Shechtman, and D. Gratias, J. Mater. Res. **1**, 13 (1986).
[8] R. Colella, Y. Zhang, J. P. Sutter, S. N. Ehrlich, and S. W. Kycia, Phys. Rev. B **63**, 014202 (2000).
[9] Y. Amazit, M. de Boissieu, and A. Zarembowitch, Europhys. Lett. **20**, 703 (1992).
[10] P. A. Kalugin, A. Yu Kitayev and L. S. Levitov, J. Phys. (France) Lett. **46**, L-601 (1985).
[11] P. Bak, Phys. Rev. B **32**, 5764 (1985).
[12] T. C. Lubensky, S. Ramaswamy, and J. Toner, Phys. Rev. B **32**, 7444 (1985).
[13] J. De Launay, in *Solid State Physics*, edited by F. Seitz and D. Turnbull (Academic Press, New York, 1956), Vol. 2, p. 220.
[14] B. E. Warren, *X-ray Diffraction* (Addison-Wesley, Reading, MA, 1969).
[15] M. V. Jarić and D. R. Nelson, Phys. Rev. B **37**, 4458 (1988).
[16] W. A. Wooster, *Diffuse X-ray Reflections from Crystals* (Clarendon Press, Oxford, 1962). See Fig. 2.2.
[17] Y. Ishii, Phys. Rev. B **45**, 5228 (1992).
[18] S. B. Rochal, Phys. Rev. B **64**, 144204 (2001).